

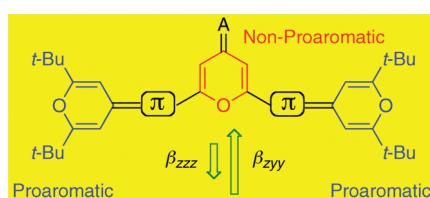
Linear and V-Shaped Nonlinear Optical Chromophores with Multiple 4*H*-Pyran-4-ylidene Moieties[§]

Raquel Andreu,[†] Elena Galán,[†] Javier Garín,^{*,†} Vanessa Herrero,[†] Edurne Lacarra,[†] Jesús Orduna,[†] Raquel Alicante,[‡] and Belén Villacampa[‡]

[†]Departamento de Química Orgánica and [‡]Departamento de Física de la Materia Condensada, ICMA, Universidad de Zaragoza-CSIC, 50009 Zaragoza, Spain

jgarin@unizar.es

Received December 16, 2009



A simple synthesis of dipolar one- and two-dimensional chromophores bearing two or three 4*H*-pyran-4-ylidene moieties is reported. Whereas the pyran-4-ylidene fragments acting as donors are proaromatic, the spacer one is not. In the linear derivatives, chain elongation gives rise to a sharp increase in the second order nonlinear optical responses, but some V-shaped derivatives display first hyperpolarizabilities (β) lower than those of their linear analogues. This uncommon feature lends experimental support to previous theoretical studies on the relative contribution and sign of the β -tensor components.

Introduction

Donor–acceptor (D–A) 4*H*-pyran-4-ylidene derivatives have attracted much attention because of their interesting optical properties. Thus, 4-dicyanomethylene-2-methyl-6-(4-dimethylaminostyryl)-4*H*-pyran (DCM) is a well-known laser dye, and many of its derivatives are useful red dopants for organic light-emitting diodes (OLED).¹ Moreover, since D–A compounds are especially relevant in the study of second order nonlinear optical (NLO) properties,² it is hardly surprising that pyran-4-ylidene-containing D–A compounds have been studied to that end.

In most cases the pyran-4-ylidene moiety is incorporated into the π -spacer, giving rise to either one-dimensional (1D) or two-dimensional (2D, also called V-shaped)³ NLO chromophores of D–A and D–A–D type, respectively.⁴

On the other hand, the 4*H*-pyran-4-ylidene fragment has been much less studied as an electron-donor in D–A compounds with NLO properties. Thus, besides theoretical studies suggesting that 4-quinopyrans with twisted intramolecular charge transfer states (and therefore, zwitterionic character) should display high first hyperpolarizability (β) values,⁵ only a few works have experimentally studied the

[§]Dedicated to Professor Antonio García Martínez on the occasion of his retirement.

(1) (a) Tang, C. W.; VanSlyke, S. A.; Chen, C. H. *J. Appl. Phys.* **1989**, *65*, 3610–3616. (b) Chen, C.-T. *Chem. Mater.* **2004**, *16*, 4389–4400. (c) Leung, M.; Chang, C.-C.; Wu, M.-H.; Chuang, K.-H.; Lee, J.-H.; Shieh, S.-J.; Lin, S.-C.; Chiu, C.-F. *Org. Lett.* **2006**, *8*, 2623–2626. (d) Yao, Y.-S.; Zhou, Q.-X.; Wang, X.-S.; Wang, Y.; Zhang, B.-W. *Adv. Funct. Mater.* **2007**, *17*, 93–100.

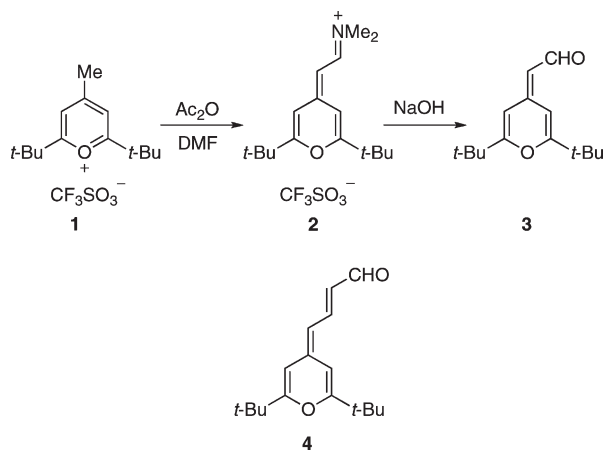
(2) (a) *Nonlinear Optics of Organic Molecules and Polymers*; Nalwa, H. S., Miyata, S., Eds.; CRC Press: Boca Raton, 1997. (b) Wolf, J. J.; Wortmann, R. *Adv. Phys. Org. Chem.* **1999**, *32*, 121–217. (c) Suponitsky, K. Yu.; Timofeeva, T. V.; Antipin, M. Yu. *Russ. Chem. Rev.* **2006**, *75*, 457–496. (d) Barlow, S.; Marder, S. R. *Nonlinear Optical Properties of Organic Materials. In Functional Organic Materials. Syntheses, Strategies, and Applications*; Müller, T. J. J., Bunz, U. H. F., Eds.; Wiley-VCH: Weinheim, 2007; pp 393–437. (e) Cho, M. J.; Choi, D. H.; Sullivan, P. A.; Akelaitis, A. J. P.; Dalton, L. R. *Prog. Polym. Sci.* **2008**, *33*, 1013–1058. (f) Marder, S. R., Guest Ed.; Themed issue on Organic Nonlinear Optics, *J. Mater. Chem.* **2009**, *19* (40).

(3) Wolff, J. J.; Wortmann, R. *J. Prakt. Chem.* **1998**, *340*, 99–111.

(4) (a) Moylan, C. R.; Ermer, S.; Lovejoy, S. M.; McComb, I.-H.; Leung, D. S.; Wortmann, R.; Krdmer, P.; Twieg, R. J. *J. Am. Chem. Soc.* **1996**, *118*, 12950–12955. (b) Illien, B.; Jehan, P.; Botrel, A.; Darchen, A.; Ledoux, I.; Zyss, J.; Le Maguères, P.; Ouahab, L. *New J. Chem.* **1998**, 633–641. (c) Jen, A. K.-Y.; Liu, Y.; Zheng, L.; Liu, S.; Drost, K.-J.; Zhang, Y.; Dalton, L. R. *Adv. Mater.* **1999**, *11*, 452–455. (d) Liu, Y.; Liu, Y.; Zhang, D.; Hu, H.; Liu, C. *J. Mol. Struct.* **2001**, *570*, 43–51. (e) Liu, Y.; Liu, Y.; Zhao, X.; Liu, C. *Int. J. Quantum Chem.* **2001**, *82*, 65–72. (f) Yang, M.; Champagne, B. *J. Phys. Chem. A* **2003**, *107*, 3942–3951. (g) Chou, S.-S. P.; Yu, C.-Y. *Synth. Met.* **2004**, *142*, 259–262. (h) Koeckelberghs, G.; De Groof, L.; Pérez-Moreno, J.; Asselberghs, I.; Clays, K.; Verbiest, T.; Samyn, C. *Tetrahedron* **2008**, *64*, 3772–3781. (i) Andreu, R.; Carrasquer, L.; Garín, J.; Modrego, M. J.; Orduna, J.; Alicante, R.; Villacampa, B.; Allain, M. *Tetrahedron Lett.* **2009**, *50*, 2920–2924.

(5) (a) Albert, I. D. L.; Marks, T. J.; Ratner, M. A. *J. Am. Chem. Soc.* **1997**, *119*, 3155–3156. (b) Albert, I. D. L.; Marks, T. J.; Ratner, M. A. *J. Am. Chem. Soc.* **1998**, *120*, 11174–11181.

SCHEME 1



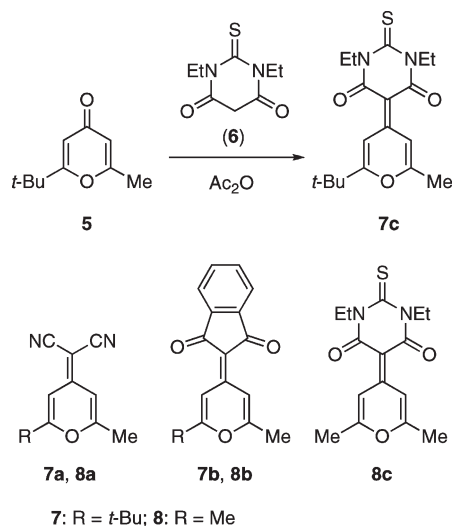
donor ability of pyranilidenes in the search for new NLO chromophores, using either organometallic⁶ or organic acceptors.⁷ The high second order NLO responses of these derivatives ultimately rely on the use of a fragment (the pyranilidene donor) gaining aromaticity on charge transfer (proaromatic), a beneficial factor first disclosed by Marder⁸ and successfully exploited later on.^{7,9}

In this paper, combining the two above-mentioned strategies, we describe the synthesis and characterization of 1D and V-shaped molecules incorporating multiple 4*H*-pyran-4-ylidene moieties (**9**–**11**), one of them acting as spacer and the other(s) as donor group(s). Experimental and theoretical evidence disclose the very different features shown by the pyranilidene rings depending on their location in the conjugated system and help explain the counterintuitive second order NLO response of the V-shaped derivatives.

Results and Discussion

Synthesis. For the synthesis of the target molecules, 4*H*-pyranilidene aldehyde **3** and its vinyllogue **4**⁷ were chosen as obvious precursors (Scheme 1). Compound **3** has been previously described, although its preparation has been

SCHEME 2



reported either to take place in very low yield (10%)¹⁰ or to give unpurified **3** in unstated yield.¹¹ Alternatively, **3** has been synthesized in 60% yield by thermolysis of not easily available dihydroxytelluranes, in turn prepared by oxidation of telluropirylium dyes.¹² We have developed a convenient, short synthesis of aldehyde **3**, by incorporating two important modifications into one of those previously reported procedures.¹¹ The first one involves the use of the easily available 2,6-di-*tert*-butyl-4-methylpyrylium triflate (**1**),¹³ which was reacted with DMF/acetic anhydride, thus avoiding the use of the potentially explosive perchlorate salt. In the second modification, the resulting iminium salt (**2**) was purified and isolated in good yield (82%). This is advantageous since salt **2** is a stable solid that, unlike the desired aldehyde, can be stored at room temperature, and its hydrolysis takes place smoothly to give **3** (83% yield).

The new acceptor **7c** was prepared from pyrone **5**¹⁴ and diethylthiobarbituric acid (**6**) in 79% yield (Scheme 2), using a similar procedure to that recently reported for the synthesis of **7a,b**.¹⁴ Concerning the remaining acceptors, **8a** is commercially available, and **8b,c** were prepared as previously described.^{4h,15,16}

The Knoevenagel reaction of the *tert*-butyl-substituted acceptors **7a**–**c** with aldehydes **3** and **4** afforded the desired 1D target compounds in medium to good yields (42–67% for **9a**–**c** and 63–79% for **11a**–**c**, Scheme 3). It is noteworthy that in the synthesis of **11c** a small amount of **9c** is also formed. This kind of degradation or vinylene-shortening reaction occurring in the preparation of relatively long merocyanines has already been reported by us^{9f,17} and others.¹⁸

(6) (a) Faux, N.; Caro, B.; Robin Le-Guen, F.; Le Poul, P.; Nakatani, K.; Ishow, E. *J. Organomet. Chem.* **2005**, *690*, 4982–4988. (b) Millán, L.; Fuentealba, M.; Manzur, C.; Carrillo, D.; Faux, N.; Caro, B.; Robin Le-Guen, F.; Sinbandhit, S.; Ledoux-Rak, I.; Hamon, J.-R. *Eur. J. Inorg. Chem.* **2006**, 1131–1138. (c) Faux, N.; Robin Le-Guen, F.; Le Poul, P.; Caro, B.; Nakatani, K.; Ishow, E.; Golhen, S. *Eur. J. Inorg. Chem.* **2006**, 3489–3497.

(7) Andreu, R.; Carrasquer, L.; Franco, S.; Garin, J.; Orduna, J.; Martínez de Baroja, N.; Alicante, R.; Villacampa, B.; Allain, M. *J. Org. Chem.* **2009**, *74*, 6647–6657.

(8) Marder, S. R.; Beratan, D. N.; Cheng, L.-T. *Science* **1991**, *252*, 103–106.

(9) (a) Abbotto, A.; Beverina, L.; Bradamante, S.; Facchetti, A.; Klein, C.; Pagani, G. A.; Redi-Abshiro, M.; Wortmann, R. *Chem.—Eur. J.* **2003**, *9*, 1991–2007. (b) Andreu, R.; Garin, J.; Orduna, J.; Alcalá, R.; Villacampa, B. *Org. Lett.* **2003**, *5*, 3143–3146. (c) Kay, A. J.; Woolhouse, A. D.; Zhao, Y.; Clays, K. *J. Mater. Chem.* **2004**, *14*, 1321–1330. (d) Andreu, R.; Blesa, M. J.; Carrasquer, L.; Garin, J.; Orduna, J.; Villacampa, B.; Alcalá, R.; Casado, J.; Ruiz-Delgado, M. C.; López-Navarrete, J. T.; Allain, M. *J. Am. Chem. Soc.* **2005**, *127*, 8835–8845. (e) Alias, S.; Andreu, R.; Blesa, M. J.; Franco, S.; Garin, J.; Gragera, A.; Orduna, J.; Romero, P.; Villacampa, B.; Allain, M. *J. Org. Chem.* **2007**, *72*, 6440–6446. (f) Alias, S.; Andreu, R.; Blesa, M. J.; Cerdán, M. A.; Franco, S.; Garin, J.; López, C.; Orduna, J.; Sanz, J.; Alicante, R.; Villacampa, B.; Allain, M. *J. Org. Chem.* **2008**, *73*, 5890–5898. (g) Schmidt, J.; Schmidt, R.; Würthner, F. *J. Org. Chem.* **2008**, *73*, 6355–6362. (h) Andreu, R.; Cerdán, M. A.; Franco, S.; Garin, J.; Marco, A. B.; Orduna, J.; Palomas, D.; Villacampa, B.; Alicante, R.; Allain, M. *Org. Lett.* **2008**, *10*, 4963–4966.

(10) Wadsworth, D. H.; Detty, M. R.; Murray, B. J.; Weidner, C. H.; Haley, N. F. *J. Org. Chem.* **1984**, *49*, 2676–2681.

(11) Wilt, J. R.; Reynolds, G. A.; Van Allan, J. A. *Tetrahedron* **1973**, *29*, 795–803.

(12) Detty, M. R. *Organometallics* **1991**, *10*, 702–712.

(13) Anderson, A. G.; Stang, P. J. *J. Org. Chem.* **1976**, *41*, 3034–3036.

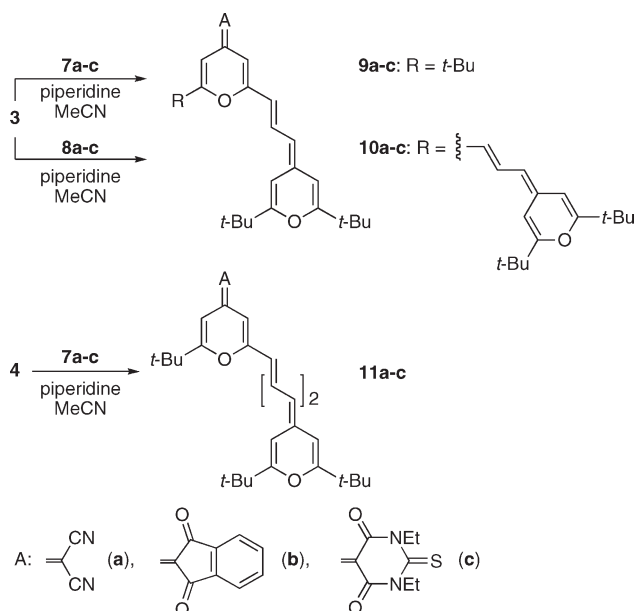
(14) Yao, Y.-S.; Xiao, J.; Wang, X.-S.; Deng, Z.-B.; Zhang, B.-W. *Adv. Funct. Mater.* **2006**, *16*, 709–718.

(15) Kelemen, J.; Wizinger, R. *Helv. Chim. Acta* **1962**, *45*, 1908–1917.

(16) Brooker, L. G. S.; Webster, F. G. U. S. Patent 2,965,486, December 20, 1960; *Chem. Abstr.* **1961**, *55*, 8131.

(17) Alias, S.; Andreu, R.; Cerdán, M. A.; Franco, S.; Garin, J.; Orduna, J.; Romero, P.; Villacampa, B. *Tetrahedron Lett.* **2007**, *48*, 6539–6542.

SCHEME 3



The V-shaped compounds **10a–c** were similarly prepared by the reaction of acceptors **8a–c** with 2 equiv of aldehyde **3** (Scheme 3). As expected for such reactions,^{4h} a small amount of the corresponding monosubstituted derivative (**9**, R = Me) was also formed, compounds **10** being purified by column chromatography.

It should be mentioned that there are very few precedents in the literature of compounds like **9–11**, in which a proaromatic donor is linked to the 2-position of a 4*H*-pyranilidene ring.^{16,19}

Structure of Precursors 2 and 3. It is noteworthy that, in our hands, the ¹H NMR spectrum of **3** in CDCl₃ is partly different from those previously reported, since the resonance signals of H-3 and H-5 of the pyran ring appear at very different chemical shifts ($\delta = 5.87$ and 7.09 ppm) and not at ca. 6.50 ppm.^{10,12} The reasons for this discrepancy remain unclear, but the ¹H NMR spectrum of **3** registered by us is in good agreement with the widely different chemical shifts of the ring hydrogen atoms at C-3 and C-5 of the thiopyran²⁰ and telluropyran²¹ analogues of **3**. Moreover, the ³J_{HH} coupling constant (6.9 Hz) of the CHO hydrogen atom reveals that the formyl group adopts an *s-trans* geometry, as opposed to the *s-cis* geometry shown by 4-acetylmethylenepyran.²² On passing, it should be noted that ¹H NMR

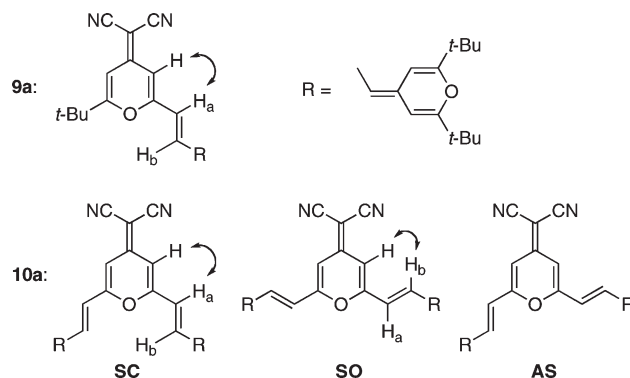


FIGURE 1. Conformers of compounds **9a** and **10a**.

data for salt **2** show the *s-trans* arrangement between the pyranilidene moiety and the iminium group, and the balanced contributions of the iminium limiting form (as depicted in the Scheme 1) and the alternative pyrylium form. In fact, the two distinct resonances of the dimethylamino group imply that the Me₂N–C bond has substantial double bond character indicative of the iminium form.²³ On the other hand, the ³J_{HH} value of ca. 12 Hz for the exocyclic vinylic hydrogen atoms of **2** is nearly identical to that found in streptocyanines²⁴ and greater than those of 3-aryl-2-propenyliideneiminium salts,²⁵ thus pointing to an appreciable contribution of the alternative pyrylium contributor. Similar considerations have been made for other hetarylidene-derived iminium salts.²⁶

Structure of Compounds 9–11. ¹H NMR and Theoretical Studies. The herein reported compounds can exist as *s-cis* or *s-trans* conformers around the bond linking the acceptor-bearing pyranilidene moiety to the polyenic spacer. Concerning the 1D-derivatives **9** and **11**, theoretical calculations show that both geometries are nearly isoenergetic (within 1 kcal/mol), and in fact, both of them have been considered in the literature for closely related dyes.^{1d,27} To study their structure in solution, we have carried out NOE experiments on compound **9a** in CDCl₃ at room temperature. They show a NOE between H_a (but not H_b) and the nearby H atom of the pyranilidene ring, thus demonstrating that **9a** exists in solution in *s-trans* geometry (Figure 1), the same displayed by the analogous compound DCM²⁸ and related derivatives in the solid state.¹⁴

On the other hand, no definitive conclusion concerning the conformational preference of the V-shaped derivatives can be reached because experiments on **10a** (at 0 °C in CDCl₃) show the existence of a NOE between the pyranilidene H atoms and both H_a and H_b, which can be interpreted as the result of a rapid equilibrium between the symmetric closed (SC), the symmetric open (SO), and the asymmetric (AS) conformers (Figure 1). Calculations also show very small

(18) (a) Alain, V.; Blanchard-Desce, M.; Ledoux-Rak, I.; Zyss, J. *Chem. Commun.* **2000**, 353–354. (b) Coe, B. J.; Harris, J. A.; Asselberghs, I.; Wostyn, K.; Clays, K.; Persoons, A.; Brunshwig, B. S.; Coles, S. J.; Gelbrich, T.; Light, M. E.; Hursthouse, M. B.; Nakatani, K. *Adv. Funct. Mater.* **2003**, *13*, 347–357. (c) Beverina, L.; Fu, J.; Leclercq, A.; Zojer, E.; Pacher, P.; Barlow, S.; Van Stryland, E. W.; Hagan, D. J.; Brédas, J.-L.; Marder, S. R. *J. Am. Chem. Soc.* **2005**, *127*, 7282–7283.

(19) (a) Van Allan, J. A.; Reynolds, G. A. *J. Heterocycl. Chem.* **1980**, *17*, 1585–1586. (b) Tolmachev, A. I.; Kachkovskii, A. D.; Kudina, M. A.; Kurdiukov, V. V.; Ksenzov, S.; Schrader, S. *Dyes Pigments* **2007**, *74*, 348–356.

(20) Young, D. N.; Detty, M. R. *J. Org. Chem.* **1997**, *62*, 4692–4700.

(21) Detty, M. R.; Young, D. N.; Williams, A. J. *J. Org. Chem.* **1995**, *60*, 6631–6634.

(22) (a) Østensen, E. T.; Undheim, K. *Acta Chem. Scand.* **1973**, *27*, 2184–2192. (b) Balaban, A. T.; Wray, V.; Furmanova, N. G.; Minkin, V. I.; Minkina, L. S.; Czernysch, Yu. E.; Borodkin, G. S. *Liebigs Ann. Chem.* **1985**, 1587–1595.

(23) Michelot, R.; Khfdua, H. *Tetrahedron* **1973**, *29*, 1031–1036.

(24) Scheibe, G.; Seiffert, W.; Hohlneicher, G.; Jutz, Ch.; Springer, H. J. *Tetrahedron Lett.* **1966**, *7*, 5053–5059.

(25) Childs, R. F.; Dickie, B. D. *J. Am. Chem. Soc.* **1983**, *105*, 5041–5046.

(26) (a) Chen, C.-T.; Marder, S. R. *Adv. Mater.* **1995**, *7*, 1030–1033.

(b) Andreu, R.; Carrasquer, L.; Cerdán, M. A.; Fernández, A.; Franco, S.; Garin, J.; Orduna, J. *Synlett* **2007**, 1470–1472.

(27) Van Tassle, A. J.; Prantil, M. A.; Fleming, G. R. *J. Phys. Chem. B* **2006**, *110*, 18989–18995.

(28) Barbon, A.; Bott, E. D.; Brustolon, M.; Fabris, M.; Kahr, B.; Kaminsky, W.; Reid, P. J.; Wong, S. M.; Wustholz, K. L.; Zanré, R. *J. Am. Chem. Soc.* **2009**, *131*, 11548–11557.

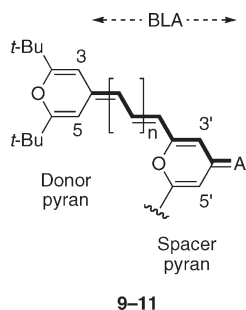


FIGURE 2. Labels for ^1H NMR data and theoretical calculations.

energy differences between these structures (up to ca. 1 kcal/mol), and therefore a marked influence of the environment (e.g., crystal, applied field, or solvent) on the conformational equilibrium can be expected.²⁹

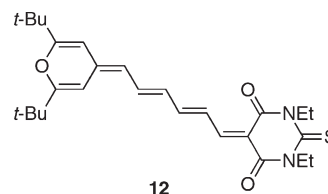
To facilitate the discussion of further structural features of compounds **9–11**, their different subunits and some relevant atoms and parameters are labeled as shown in Figure 2, where BLA (bond length alternation)³⁰ stands for the difference between the average C–C and C=C bond lengths along the spacer (indicated in bold).

The proaromaticity of the 4*H*-pyran-4-ylidene donor moiety in polyene-linked D–A compounds has recently been demonstrated.⁷ Similarly, the so-called donor pyran fragment(s) of derivatives **9–11** have proaromatic character, as shown by ^1H NMR data and theoretical calculations. Thus, H-3 and H-5 of that ring in compounds **9** appear at δ values similar to those displayed by the corresponding H atoms in linear polyenic analogues of the same conjugation length.⁷ The observed upfield shift for such protons on passing from compounds **9** to **11** reveals a decrease in the aromatic (zwitterionic) contribution on lengthening the spacer, since H-3 and H-5 of the pyranlydene ring are known to undergo downfield shifts as the pyrylium character of the ring increases.^{6b,26a} Similarly, those H atoms in compounds **10** have slightly lower δ values than those of the corresponding 1D-derivatives **9**, thus pointing to a lower aromatic character for the donor pyran rings of the V-shaped compounds.

The acyclic polyenic fragments linking the pyranlydene subunits of compounds **9–11** have a merocyanine-like character since their polymethinic H atoms show an oscillatory behavior of their chemical shifts^{24,31} and ΔJ values in the range 2.2–2.6 Hz (ΔJ , defined as the difference between the averaged $^3J_{\text{HH}}$ values of the double and single bonds along the polymethine chain,³² ranges from 0 Hz in cyanines to ca. 6 Hz in polyenes).^{24,33} Compounds **9** show lower ΔJ values than **10–11**, thus confirming the higher proaromatic character of the donor pyran in the former derivatives. Furthermore, a comparison of compounds **9** with their analogues featuring acyclic polyenic spacers reveals that the latter have much lower

ΔJ values (≤ 1 Hz)⁷ and therefore more polarized ground states, an hypothesis that is also supported theoretically.

Thus, calculations on thiobarbiturate derivatives **9c–11c** reveal a low BLA value for **9c** (0.037 Å), which slightly increases on lengthening the spacer (**11c**, BLA = 0.041 Å). Similarly, **10c** has a BLA value (0.039 Å) higher than that of **9c**. Furthermore, the noticeably lower BLA value of the linear analogue **12** (0.031 Å) shows that the introduction of the pyranlydene moiety into the polyenic spacer results in a more alternated structure with a less efficient conjugation between the donor and acceptor ends of the molecule. This is in good agreement with the aromaticity of the pyranlydene ring of **12**, which as calculated by its Bird index³⁴ ($I_6 = 39.8$) is higher than that of the donor pyran ring of **9c** ($I_6 = 38.4$).



The remaining acceptors (series **a** and **b**) show features similar to those of **c**, although the slightly increased ΔJ values (2.5–2.6 Hz) of compounds **b** suggest a comparatively weaker electron-withdrawing effect of the indanedione acceptor, which is confirmed by the decrease of BLA values in the series: **b** > **a** > **c**.

Concerning the spacer pyran ring, its H atoms (H-3' and H-5', see Figure 2) are progressively shielded on increasing the number of donor chains (for instance, their δ values decrease in the series **7c** > **9c** > **10c**). This shielding effect caused by the donor pyran group slightly decreases on increasing the spacer length, giving rise to higher δ values for those protons in compounds **11** than in **9**.

The calculated geometries of the spacer pyrans in the nonsymmetrical derivatives **9** and **11** show that there is a much lower degree of bond length alternation on the donor-containing side (as measured by the (*a* – *b*) parameter) than on the other side (*c* – *d*), as exemplified in Figure 3 for compounds **c**.

	compd	(<i>a</i> – <i>b</i>)	(<i>c</i> – <i>d</i>)
	9c : R = <i>t</i> -Bu	0.047	0.089
	11c : R = <i>t</i> -Bu	0.049	0.089
	10c : R = D	0.052	0.052

FIGURE 3. Selected bonds and bond length differences (in Å) in the spacer pyran.

This asymmetry, also found in the solid-state structure of DCM,²⁸ strongly suggests (i) that the zwitterionic form **II** (Figure 4) is not a relevant contributor, thus ruling out the proaromaticity of this ring, and (ii) that there is an important participation of the merocyanine-like form **III** to the description of these molecules, the contribution of form **IV** being more limited. Moreover, when different acceptors are compared, the fact that (*a* – *b*) decreases in the order **b** > **a** > **c** suggests that the thiobarbiturate is the strongest acceptor.

(29) Chang, P.-H.; Chen, J.-Y.; Tsai, H.-C.; Hsiue, G.-H. *J. Polym. Sci., Part A: Polym. Chem.* **2009**, *47*, 4937–4949.

(30) Marder, S. R.; Perry, J. W.; Tiemann, B. G.; Gorman, C. B.; Gilmour, S.; Biddle, S. L.; Bourhill, G. *J. Am. Chem. Soc.* **1993**, *115*, 2524–2526.

(31) Kulinich, A. V.; Ishchenko, A. A.; Groth, U. M. *Spectrochim. Acta, Part A* **2007**, *68*, 6–14.

(32) Marder, S. R.; Perry, J. W.; Bourhill, G.; Gorman, C. B.; Tiemann, B. G.; Mansour, K. *Science* **1993**, *261*, 186–189.

(33) Blanchard-Desce, M.; Alain, V.; Bedworth, P. V.; Marder, S. R.; Fort, A.; Runser, C.; Barzoukas, M.; Lebus, S.; Wortmann, R. *Chem.—Eur. J.* **1997**, *3*, 1091–1104.

(34) (a) Bird, C. W. *Tetrahedron* **1985**, *41*, 1409–1414. (b) Bird, C. W. *Tetrahedron* **1986**, *42*, 89–92.

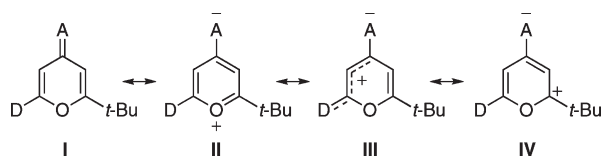


FIGURE 4. Some limiting forms of compounds **9** and **11**.

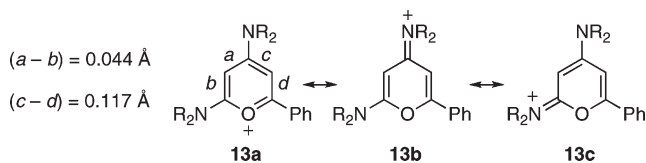


FIGURE 5. Related 2,4-bis(dialkylamino)pyrylium salts.

2,4-Bis(dialkylamino)pyrylium salts (**13**) represent a closely related situation, since X-ray diffraction data³⁵ and NMR measurements³⁶ indicate a predominance of the vinylidinium limiting forms (**13b**, **13c**) over the pyrylium form (**13a**) (Figure 5).

In a similar way, symmetrical compounds **10** show low ($a - b$) values, and this relative bond length equalization must be essentially due to the strong interactions between the 4-acceptor group and the 2- and 6-donor groups through the pyran spacer since, on replacement of the donor groups by methyl substituents (Figure 6), the decrease in ($a - b$) is much lower and can only be attributed to the proaromaticity of the pyran ring (e.g., for **10a**, ($a - b$) = 0.056 Å, whereas for its dimethyl analogue **14** bearing the same acceptor, ($a - b$) = 0.082 Å).⁴ⁱ

Therefore, compounds **10** should be best viewed as cross-conjugated merocyanines. Dipole moment measurements,³⁷ theoretical calculations³⁷ and NMR experiments^{36b,c} on 2,6-diamino- γ -pyrones, and UV-vis spectra of related ketocyanines³⁸ have also been interpreted along similar lines. Taken together, all of these results clearly signal that, unlike the donor pyran ring(s), the spacer pyrans of compounds **9–11** do not have a noticeable proaromatic character.

Electrochemistry. The electrochemical properties of **9–11** were determined by cyclic voltammetry. Most of these derivatives show one irreversible oxidation wave and one reversible reduction wave (table 1).

When compounds **9** and **11** are compared, it can be seen that lengthening the spacer gives rise to a cathodic (anodic) shift of the oxidation (reduction) potentials, pointing to a weaker interaction between the donor and acceptor end-groups for the longer derivatives. This is in good agreement with the higher HOMO energies and the lower LUMO energies of compounds **11**. Concerning compounds **10**, it is noteworthy that even though they show E_{ox} values similar to those of **9**, they are also easier to reduce. Moreover, a comparison of the LUMO energy values in any series

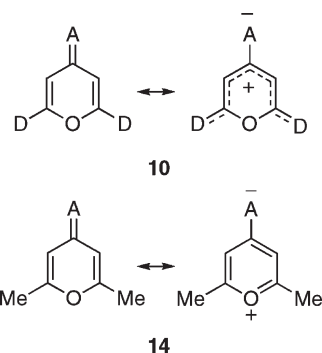


FIGURE 6. Limiting forms of compounds **10** and their 2,6-dimethyl analogues **14**.

(**9–11**) points to the fact that the thiobarbiturate group is the strongest acceptor among those employed in this work.

UV-vis Spectroscopy. UV-vis spectra show that, for any series of compounds (**9**, **10** or **11**), λ_{max} values decrease in the following order: $c > b > a$. This trend is in good agreement with previous observations on pyranlydene-based chromophores^{4g,i} and confirms that the thiobarbiturate group is the strongest of the herein studied acceptors. Concerning the effect of chain lengthening, there is a noticeable bathochromic shift on passing from compounds **9** to **11** (see Supporting Information). The magnitude of this vinylenic shift is nevertheless small (ca. 20 nm), a situation reminiscent of that found in pyrane-containing merocyanines with low-basicity donor end groups.^{19b} In good agreement with previous experimental^{4g-i} and theoretical results,^{4e,i} 2D compounds **10** show red-shifted absorptions when compared to their 1D analogues **9**. It is noteworthy that unlike **10a,b**, which show strongly overlapped bands, **10c** shows clearly resolved bands, a distinctive feature supported by theoretical calculations (see below). Finally, compounds **9**, **10**, and **11** show positive solvatochromism. This behavior has been encountered a number of times for 1D^{4i,19b,39} and V-shaped pyran chromophores⁴ⁱ and can be traced back to the increase in dipole moment associated to the lowest energy transition.⁴⁰

Nonlinear Optical Properties. The second order nonlinear optical properties of compounds **9–11** were measured by electric field-induced second harmonic generation (EFISH) at 1,907 nm in dichloromethane, and the static (zero-frequency) $\mu\beta_0$ values were calculated by the two-level model⁴¹ for the sake of comparison Disperse Red 1, a common benchmark of organic NLO-chromophores, gives a $\mu\beta_0$ value of ca. 480×10^{-48} esu in the same experimental conditions). Since the two-level model is a valid approximation only for compounds with a single low-energy ICT transition, the $\mu\beta_0$ values reported in Table 2 are reliable for compounds **11** but only approximate for compounds **9**. Moreover, the spectral features of compounds **10** preclude the calculation of well-founded $\mu\beta_0$ values for the V-shaped derivatives. In any case, Table 2 reveals that for each series of compounds (**9–11**), dicyanomethylene and thiobarbituric

(35) Barnes, J. C.; Paton, J. D.; Spitzner, R.; Schroth, W. *Tetrahedron* **1990**, *46*, 2935–2942.

(36) (a) Kleinpeter, E.; Spitzner, R.; Schroth, W. *Magn. Reson. Chem.* **1987**, *25*, 688–695. (b) Kleinpeter, E.; Spitzner, R.; Schroth, W.; Pihlaja, K.; Mattinen, J. *Magn. Reson. Chem.* **1988**, *26*, 707–713. (c) Kleinpeter, E.; Spitzner, R.; Peters, A.; Schroth, W.; Pihlaja, K. *J. Prakt. Chem.* **1990**, *332*, 313–318.

(37) Schroth, W.; Spitzner, R.; Minkin, V. *J. Phys. Org. Chem.* **1993**, *6*, 489–493.

(38) Krasnaya, Z. A.; Smirnova, Y. V.; Tatikolov, A. S.; Kuz'min, V. A. *Russ. Chem. Bull.* **1999**, *48*, 1329–1334.

(39) Boldrini, B.; Cavalli, E.; Painelli, A.; Terenziani, F. *J. Phys. Chem. A* **2002**, *106*, 6286–6294.

(40) (a) Meyer, M.; Mialocq, J. C. *Opt. Commun.* **1987**, *64*, 264–268. (b) Khohlova, S. S.; Lebedev, N. G.; Bondarev, S. L.; Knyukshto, V. N.; Turban, A. A.; Mikhailova, V. A.; Ivanov, A. I. *Int. J. Quantum Chem.* **2005**, *104*, 189–196.

(41) Kanis, D. R.; Ratner, M. A.; Marks, T. *J. Chem. Rev.* **1994**, *94*, 195–242.

TABLE 1. Electrochemical Data,^a E_{HOMO} and E_{LUMO} Values^b (eV), and UV-vis Data

compd	E_{ox}	$E_{\text{red}}^{1/2}$	E_{HOMO}	E_{LUMO}	λ_{max} (CH ₂ Cl ₂) (log ϵ)	λ_{max} (DMSO)
9a	+0.80	-1.34 (0.12)	-5.75	-2.98	519 (4.72), 558 (sh)	526
9b	+0.72	-1.26 (0.10)	-5.52	-2.78	547 (4.74), 577 (sh)	559
9c	+0.76	-1.18 (0.11)	-5.72	-3.03	587 (4.52)	593
10a	+0.83	-1.12 (0.13)	-5.50	-2.81	522 (4.70), 574 (sh)	527, 582 (sh)
10b	+0.74	-1.19 (0.15)	-5.29	-2.68	552 (4.64), 614 (sh)	560, 631 (sh)
10c	+0.72	-1.12 (0.12), -1.91 ^c	-5.40	-2.89	552 (4.87), 633 (4.64)	561, 658
11a	+0.55	-1.28 (0.11)	-5.60	-3.09	543 (4.76)	555
11b	+0.53	-1.18 (0.11)	-5.39	-2.89	572 (4.68)	587
11c	+0.59	-1.21 ^c	-5.56	-3.12	602 (4.70)	619

^aIn volts, 10⁻³ M in CH₂Cl₂ vs Ag/AgCl (KCl 3 M), glassy carbon working electrode, Pt counter electrode, 20 °C, 0.1 M Bu₄NPF₆, 100 mV s⁻¹ scan rate. Peak-to-peak separation (ΔE_{p} , in volts) in parentheses. Ferrocene internal reference $E^{1/2} = +0.43$ V ($\Delta E_{\text{p}} = 0.17$). ^bCalculated in the gas phase at the B3P86/6-31G*//B3P86/6-31G* level for the geometries shown in Figure 1 (AS conformer for compounds **10a–c**). ^cIrreversible wave.

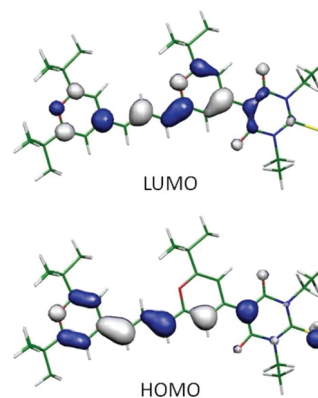
TABLE 2. Experimental^a and Calculated^b NLO Properties

compd	experimental		conformer ^f	CPHF ^c			TDDFT ^d			
	$\mu\beta^e$	$\mu\beta_0^e$		$\mu\beta_0^g$	β_{zzz}^h	β_{zyy}^h	E (eV)	symmetry	f	$\Delta\mu_{\text{gc}}$ (D)
9a	1070	698		415			2.78		1.57	2.34
9b	860	529		249			2.64		1.75	7.18
9c	1160	652		380			2.57		1.68	3.90
10a	900		SC	-107	-46	41	2.34	B	0.26	5.53
			SO	658	-13	74	2.43	B	0.64	0.29
						2.52	A	0.08	-3.53	
10b	670		SC	-228	-64	48	2.27	B	0.33	8.03
			SO	317	-20	84	2.38	B	1.31	4.17
						2.45	A	0.70	-1.51	
10c	1500		SC	-370	-76	58	2.47	A	0.23	-3.31
			SO	757	-25	95	2.18	B	0.38	7.49
						2.41	A	0.71	-4.92	
						2.30	B	1.53	3.98	
						2.46	A	0.21	-5.65	
11a	2630	1633		1939			2.55		2.06	7.48
11b	1600	932		1079			2.45		2.18	11.30
11c	2530	1370		2043			2.38		2.09	9.37

^aIn CH₂Cl₂ at 1907 nm. ^bOn B3P86/6-31G* geometries. ^cCPHF/6-31G* level. ^dB3P86/6-31G* level. ^eIn 10⁻⁴⁸ esu. Experimental accuracy: $\pm 10\%$. ^fSee Figure 1. ^gIn 10⁻⁴⁸ esu. ^hIn 10⁻³⁰ esu.

derivatives show $\mu\beta$ values higher than those of their indanedione analogues, thus confirming the weaker electron-withdrawing ability of the latter acceptor.

When 1D compounds (**9** and **11**) are compared, it can be seen that lengthening the polyenic chain by a single vinylene unit gives rise to an important increase in the second order NLO response, the $\mu\beta$ values of compounds **11** being roughly double those of **9**. Coupled-perturbed Hartree-Fock (CPHF) calculations qualitatively reproduce the experimentally observed trends, although the calculated $\mu\beta_0$ values of compounds **9** (**11**) are systematically underestimated (overestimated). Moreover, TDDFT calculations provide a better understanding of the factors responsible for the NLO response, since they afford the parameters involved in the two-level model. In this approach, $\beta_0 \propto \Delta\mu_{\text{gef}}/E^3$, where $\Delta\mu_{\text{gc}}$ is the difference between the excited- and ground-state dipole moments (μ_e and μ_g , respectively), f is the oscillator strength, and E is the excitation energy. The increase in $\Delta\mu_{\text{gc}}$ and f , together with the decrease in E on lengthening of the spacer, readily accounts for the higher $\mu\beta_0$ values of **11** when compared with those of **9**. TDDFT calculations show that most of the experimental hyperpolarizability (β) in these 1D derivatives is accounted for by the intense, low-lying HOMO \rightarrow LUMO transition. Such orbitals, exemplified for **9c** in Figure 7, show that, on excitation, electron density is essentially transferred from the donor pyran ring to the spacer pyran and not to the thiobarbituric moiety.

**FIGURE 7.** Frontier orbitals of **9c**.

This counterintuitive result is confirmed by the variation in the Mulliken charges of the different molecular fragments upon excitation (Δq , Table 3), which reveals that in these compounds the alleged acceptor becomes a weak donor.

2D compounds **10** (except **10c**) show experimental $\mu\beta$ values lower than those of their 1D-analogues **9** of the same length. This is at first sight surprising since the opposite trend has been repeatedly reported,^{4a,d,g-1} but theoretical calculations shed some light on the optical properties of compounds **10**. CPHF and TDDFT calculations on the quasi-isoenergetic *C*₂ conformers **SO** and **SC** of **10** (Figure 1) have been

TABLE 3. Variation in Mulliken Charges (Δq) (e) on Excitation

compd	transition	donor pyran + polyenic spacer	spacer pyran	thiobarbituric
9c	HOMO \rightarrow LUMO	+0.27	-0.32	+0.05
10c	HOMO \rightarrow LUMO	+0.13 ^a	-0.16	-0.11
10c	HOMO-1 \rightarrow LUMO	+0.02 ^a	-0.21	+0.17

^a Δq value for each (donor pyran + polyenic spacer) fragment in the SO conformer.

carried out with the molecules lying in the yz plane and taking the C_2 axis as the z direction. In such orientation, only two components of the β tensor have to be taken into account, β_{zzz} (“diagonal”) and β_{zyy} (“off-diagonal”), being the EFISH-sampled component $\beta_{\text{vec}} = \beta_z = \beta_{zzz} + \beta_{zyy}$. Table 2 reveals that CPHF-calculated β_z values are always negative for the SC conformers. On the other hand, the calculated β_z (and hence, $\mu\beta$ values) for the SO conformers are in better agreement with the experimental ones, and therefore most of the following discussion will make use of this geometry. According to CPHF calculations, β_{zyy} values of compounds **10** are always positive, whereas β_{zzz} are negative, and given that for the SO conformers $|\beta_{zyy}| > |\beta_{zzz}|$, they are calculated to show positive β values. The fact that $\beta_{zyy} > 0$ is in good agreement with previous reports on related V-shaped pyranilidene derivatives,^{4a,f,i} but β_{zzz} , instead of contributing to β in an additive fashion,^{4a} is negative, a situation that had been theoretically predicted by Champagne.^{4f} It is noteworthy that CPHF calculations predict larger $\mu\beta_0$ values for the SO conformers of compounds **10** than for **9**, in marked contrast to the experimental results for **9a/10a** and **9b/10b**. This seeming contradiction can be solved taking into account the existence of SC conformers in the conditions of the EFISH experiments since, as a result of their larger negative β_{zzz} values, they contribute in a negative fashion to the experimentally observed $\mu\beta$ values.

TDDFT calculations (Table 2) show that for the SO conformers the lowest-lying transition is polarized perpendicular to the C_2 axis (B symmetry), whereas the second one is polarized parallel to it (A symmetry). The former, with a positive $\Delta\mu_{\text{ge}}$ value and high oscillator strength, is associated with the off-diagonal component (β_{zyy}), whereas the latter, with a negative $\Delta\mu_{\text{ge}}$ value and lower f is at the origin of the comparatively smaller and negative β_{zzz} value. The larger absolute values of β_{zyy} compared with β_{zzz} can be traced back to the large angle between the two charge transfer axes.^{4f} This angle (defined as that formed by the two lines passing through the oxygen atoms of the donor pyrans and the carbon atom of the acceptor linked to the spacer pyran) is very high for the SO conformers (e.g., for **10c**, 131°), whereas SC conformers display much lower angles (44° for **10c**) and therefore show decreased (increased) β_{zyy} (β_{zzz}) values.

The lowest transition in compounds **10** is HOMO \rightarrow LUMO, and Figure 8 shows for **10c** that, on excitation, electron density is transferred from the donor wings to the spacer pyran and the thiobarbituric moiety.

On the other hand, the next transition contributing to β is HOMO-1 \rightarrow LUMO, giving rise to a charge transfer from the thiobarbituric fragment to the spacer pyran (see Table 3) and therefore to negative β_{zzz} values. It is noteworthy that, according to previous studies,^{4f} such negative values are indicative of strong donor/acceptor pairs, thus providing

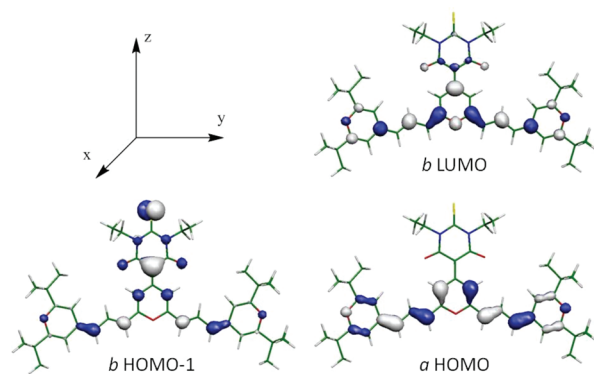


FIGURE 8. Orbitals of **10c** involved in the lowest energy electronic transitions.

an additional indication of the strong donating ability of the proaromatic pyranilidene rings. On passing, it should be noted that TDDFT calculations (Table 2) predict a larger relative gap between the two lowest energy transitions of **10c** when compared with **10a** and **10b**, correlating with the observed UV-vis spectra.

Although for the sake of simplicity the previous discussion has focused on the symmetric conformers of **10**, CPHF calculations on the slightly more stable AS conformers (Figure 1) have also been carried out and provide $\mu\beta_0$ values (**10a**, 623×10^{-48} esu; **10b**, 311×10^{-48} esu; **10c**, 668×10^{-48} esu) similar to those of the SO conformers.

Finally, it is worth noting that the donor ability of the proaromatic pyranilidene fragment is similar to that of the *N,N*-diethylanilino group, as judged from the $\mu\beta_0$ values of the corresponding 1D derivatives.⁴ⁱ On the other hand, when 2D compounds are compared, the anilino analogues show in most cases higher $\mu\beta$ values because of the opposite contribution of β_{zyy} and β_{zzz} to the NLO response of compounds **10**.

To sum up, linear (D-A) and V-shaped (D-A-D) NLO-chromophores bearing multiple 4*H*-pyran-4-ylidene moieties have been prepared for the first time. Unlike the donor pyranilidene fragments, the spacer pyranilidenes do not show noticeable proaromatic character. The strong acceptor character of the spacer pyran ring on excitation is responsible for the negative diagonal hyperpolarizability (β_{zzz}) values of the 2D compounds herein studied, which in some cases give rise to lower second order NLO responses compared with those of their 1D-counterparts. This unusual behavior can be accounted for by the different signs of the diagonal and the off-diagonal components of β , which had been predicted on theoretical grounds.

Experimental Section

Compounds **1**,¹³ **4**,⁷ **5**,¹⁴ **7a-b**,¹⁴ **8b**,^{15,42} and **8c**¹⁶ were prepared as previously described.

***N,N*-Dimethyl 2-(2,6-Di-*tert*-butyl-4*H*-pyran-4-ylidene)ethylideniminium Triflate (2)**. To a refluxed solution of 2,6-di-*tert*-butyl-4-methylpyrilium triflate (**1**) (2.9 g, 8.15 mmol) in acetic anhydride (29 mL) was added anhydrous DMF (2.9 mL, 37 mmol) under argon. The mixture was refluxed for 15 min,

(42) Kim, D. U.; Paik, S.-H.; Kim, S.-H.; Tak, Y.-H.; Han, Y.-S.; Kim, S.-D.; Kim, K.-B.; Ju, H.-J.; Kim, T.-J. *Mater. Sci. Eng., C* **2004**, *24*, 147-149.

then allowed to cool to room temperature, and finally poured into ice-cooled Et₂O (250 mL). The resulting green solid was isolated by filtration, washed with cold Et₂O and dried, to afford the iminium salt **2** (2.75 g, 82%). Mp 258–260 °C. IR (Nujol, cm⁻¹) 1606 (C=N). ¹H NMR (CDCl₃, 400 MHz): δ 8.72 (d, *J* = 12.2 Hz, 1H), 7.27 (d, *J* = 1.8 Hz, 1H), 6.41 (d, *J* = 1.8 Hz, 1H), 5.42 (d, *J* = 12.2 Hz, 1H), 3.56 (s, 3H), 3.18 (s, 3H), 1.36 (s, 9H), 1.31 (s, 9H). ¹³C NMR (CDCl₃, 100 MHz): δ 174.4, 174.1, 159.3, 158.1, 122.4, 108.4, 102.7, 98.5, 47.1, 38.6, 37.1, 36.6, 27.9, 27.1. MS (MALDI⁺): *m/z* 262 [C₁₇H₂₈NO]⁺. Anal. Calcd for C₁₈H₂₈F₃NO₄S: C 52.54, H 6.86, N 3.40. Found: C 52.29, H 7.03, N 3.11.

2,6-Di-tert-butyl-4-formylmethylene-4H-pyran (3). To a solution of salt **2** (493 mg, 1.2 mmol) in CH₂Cl₂ (10 mL) was added aqueous NaOH 10% (1.08 mL, 2.5 equiv). The mixture was stirred at room temperature for 7 h. Then, a second portion of NaOH (2.16 mL, 5 equiv) was added, and the reaction was stirred overnight. CH₂Cl₂ (50 mL) was added, and the organic layer was washed with water (3 × 100 mL), dried (MgSO₄) and evaporated. A pale yellow oil (234 mg, 83%) was obtained. The product can be used without further purification, but as soon as possible. ¹H NMR (CDCl₃, 400 MHz): δ 9.74 (d, *J* = 6.9 Hz, 1H), 7.09 (br s, 1H), 5.87 (d, *J* = 1.8 Hz, 1H), 5.32 (d, *J* = 6.9 Hz, 1H), 1.24 (s, 9H), 1.22 (s, 9H). ¹H NMR (DMSO-*d*₆, 300 MHz): δ 9.78 (d, *J* = 7.4 Hz, 1H), 7.11 (s, 1H), 6.12 (d, *J* = 1.8 Hz, 1H), 5.33 (d, *J* = 7.4 Hz, 1H), 1.23 (s, 9H), 1.20 (s, 9H). ¹³C NMR (CDCl₃, 100 MHz): δ 187.6, 168.8, 168.7, 148.5, 109.5, 105.0, 99.8, 36.2, 36.0, 27.9, 27.8. HRMS (ESI⁺): calcd for C₁₅H₂₃O₂ (M + H)⁺ 235.1693; found 235.1687; calcd for C₁₅H₂₂NaO₂ (M + Na)⁺ 257.1512; found 257.1510. Anal. Calcd for C₁₅H₂₂O₂: C 76.88, H 9.46. Found: C 76.41, H 9.07.

5-(2-tert-Butyl-6-methyl-4H-pyran-4-ylidene)-1,3-diethyl-2-thioxodihydropyrimidine-4,6-dione (7c). A solution of 2-tert-butyl-6-methyl-4H-pyran-4-one (**5**) (500 mg, 3 mmol) and 1,3-diethylthioimbarbituric acid (**6**) (600 mg, 3 mmol) in acetic anhydride (4.5 mL) was refluxed under argon atmosphere for 2.5 h. The reaction mixture was allowed to reach room temperature, and the resulting solid was filtered off, washed with cold methanol and dried. A yellow solid was obtained (825 mg, 79%). Mp 179–181 °C. IR (Nujol, cm⁻¹) 1132 (C=S), 1667 (C=O). ¹H NMR (CDCl₃, 400 MHz): δ 8.96 (d, *J* = 2.0 Hz, 1H), 8.80–8.79 (m, 1H), 4.58 (q, *J* = 6.8 Hz, 4H), 2.49 (d, *J* = 0.3 Hz, 3H), 1.37 (s, 9H), 1.31 (t, *J* = 6.8 Hz, 6H). ¹³C NMR (CDCl₃, 100 MHz): δ 177.7, 175.8, 165.5, 161.8, 158.8, 111.7, 108.1, 96.9, 43.2, 37.0, 28.2, 20.7, 12.5. HRMS (ESI⁺): calcd for C₁₈H₂₅N₂O₃S (M + H)⁺ 349.1580; found 349.1590; calcd for C₁₈H₂₄N₂NaO₃S (M + Na)⁺ 371.1400; found 371.1397. Anal. Calcd for C₁₈H₂₄N₂O₃S: C 62.04, H 6.94, N 8.04. Found: C 62.33, H 7.24, N 7.87.

Compounds 9a–c. General Procedure. To a solution of aldehyde **3** (234 mg; 1 mmol) and the corresponding pyranone derivative (**7a–c**) (1 mmol) in acetonitrile (15 mL) was added piperidine (0.11 mL; 1.1 mmol). The mixture was refluxed under argon atmosphere with exclusion of light for 7–20 h (TLC monitoring). After cooling, the solvent was distilled, and CH₂Cl₂ was added (100 mL). The organic layer was washed with HCl 0.1 M (2 × 100 mL) and water (2 × 100 mL) and dried (MgSO₄), and the solvent evaporated. The crude product was purified by column chromatography on silica gel.

(E)-(2-tert-Butyl-6-(3-(2,6-di-tert-butyl-4H-pyran-4-ylidene)prop-1-enyl)-4H-pyran-4-ylidene)malononitrile (9a). Reaction time: 16 h. Chromatography eluent: hexane/AcOEt (85:15). Yield: purple solid (288 mg; 67%). Mp 204–207 °C. IR (Nujol, cm⁻¹) 2198 (C≡N). ¹H NMR (CDCl₃, 400 MHz): δ 7.52 (dd, *J* = 14.6 Hz, *J'* = 12.3 Hz, 1H), 6.45 (d, *J* = 2.0 Hz, 1H), 6.43 (d, *J* = 2.0 Hz, 1H), 6.17 (d, *J* = 1.7 Hz, 1H), 5.88 (d, *J* = 14.6 Hz, 1H), 5.79 (d, *J* = 1.7 Hz, 1H), 5.58 (d, *J* = 12.3 Hz, 1H), 1.34 (s, 9H), 1.24 (s, 9H), 1.21 (s, 9H). ¹³C NMR (CDCl₃,

100 MHz): δ 171.2, 166.2, 166.1, 160.9, 156.5, 139.8, 134.4, 116.3, 116.2, 112.9, 109.9, 105.2, 104.1, 102.0, 98.5, 56.1, 36.4, 35.8, 35.6, 28.1, 27.7, 27.6. HRMS (ESI⁺): calcd for C₂₈H₃₅N₂O₂ (M + H)⁺ 431.2693; found 431.2697. Anal. Calcd for C₂₈H₃₄N₂O₂: C 78.10, H 7.96, N 6.51. Found: C 78.37, H 8.19, N 6.40.

(E)-2-(2-tert-Butyl-6-(3-(2,6-di-tert-butyl-4H-pyran-4-ylidene)prop-1-enyl)-4H-pyran-4-ylidene)-1,3-indanedione (9b). Reaction time: 20 h. Chromatography eluent: hexane/AcOEt (85:15). Yield: maroon solid (342 mg; 67%). Mp 114–116 °C. IR (Nujol, cm⁻¹) 1666 (C=O). ¹H NMR (CDCl₃, 400 MHz): δ 8.37 (d, *J* = 1.7 Hz, 1H), 8.25 (d, *J* = 1.7 Hz, 1H), 7.72–7.68 (m, 2H), 7.56–7.54 (m, 3H), 6.19 (d, *J* = 1.7 Hz, 1H), 6.06 (d, *J* = 14.7 Hz, 1H), 5.77 (d, *J* = 1.7 Hz, 1H), 5.61 (d, *J* = 12.2 Hz, 1H), 1.40 (s, 9H), 1.24 (s, 9H), 1.21 (s, 9H). ¹³C NMR (CDCl₃, 100 MHz): δ 192.9, 172.9, 165.8, 165.6, 163.3, 149.8, 140.6, 140.5, 138.9, 133.3, 132.7, 120.9, 120.8, 115.0, 110.4, 107.2, 106.7, 105.2, 103.1, 98.9, 36.7, 35.8, 35.6, 28.3, 27.8, 27.7. HRMS (ESI⁺): calcd for C₃₄H₃₉O₄ (M + H)⁺ 511.2843; found 511.2839. Anal. Calcd for C₃₄H₃₈O₄: C 79.97, H 7.50. Found: C 79.72, H 7.76.

(E)-5-(2-tert-Butyl-6-(3-(2,6-di-tert-butyl-4H-pyran-4-ylidene)prop-1-enyl)-4H-pyran-4-ylidene)-1,3-diethyl-2-thioxodihydropyrimidine-4,6-dione (9c). Reaction time: 7.5 h. Chromatography eluent: CH₂Cl₂. Yield: dark blue solid (237 mg; 42%). Mp 203–205 °C. IR (Nujol, cm⁻¹) 1661 (C=O), 1132 (C=S). ¹H NMR (CDCl₃, 400 MHz): δ 8.70 (d, *J* = 1.9 Hz, 1H), 8.68 (d, *J* = 1.9 Hz, 1H), 7.66 (dd, *J* = 14.6 Hz, *J'* = 12.4 Hz, 1H), 6.24 (d, *J* = 1.7 Hz, 1H), 6.07 (d, *J* = 14.6 Hz, 1H), 5.83 (d, *J* = 1.7 Hz, 1H), 5.63 (d, *J* = 12.4 Hz, 1H), 4.60 (q, *J* = 6.9 Hz, 4H), 1.42 (s, 9H), 1.32 (t, *J* = 6.9 Hz, 6H), 1.26 (s, 9H), 1.22 (s, 9H). ¹³C NMR (CDCl₃, 100 MHz): δ 177.4, 173.0, 166.6, 166.5, 164.4, 161.9, 157.9, 140.5, 135.1, 114.5, 111.6, 110.6, 107.6, 105.6, 99.2, 96.0, 43.3, 37.0, 35.9, 35.7, 28.5, 27.8, 27.7, 12.6. HRMS (ESI⁺): calcd for C₃₃H₄₅N₂O₄S (M + H)⁺ 565.3095; found 565.3082. Anal. Calcd for C₃₃H₄₄N₂O₄S: C 70.18, H 7.85, N 4.96. Found: C 69.85, H 7.61, N 5.22.

Compounds 10a–c. General Procedure. To a solution of aldehyde **3** (234 mg; 1 mmol) and the corresponding pyranone derivative (**8a–c**) (0.476 mmol) in acetonitrile (7.5 mL) was added piperidine (0.1 mL; 1 mmol). The mixture was refluxed under argon atmosphere with exclusion of light for 24 h. After cooling, acetonitrile was distilled, and CH₂Cl₂ was added (100 mL). The organic layer was washed with HCl 0.1 M (2 × 100 mL) and water (2 × 100 mL) and dried (MgSO₄), and the solvent was evaporated. The crude product was purified by flash chromatography on silica gel.

(2,6-Bis((E)-3-(2,6-di-tert-butyl-4H-pyran-4-ylidene)prop-1-enyl)-4H-pyran-4-ylidene)malononitrile (10a). Chromatography eluent: hexane/AcOEt (9:1). Yield: dark maroon solid (52 mg; 18%). Mp 213–217 °C (dec). IR (Nujol, cm⁻¹) 2201, 2184 (C≡N), 1621 (C=C). ¹H NMR (CDCl₃, 400 MHz): δ 7.42 (dd, *J* = 14.7 Hz, *J'* = 12.1 Hz, 1H), 6.47 (s, 1H), 6.15 (d, *J* = 1.7 Hz, 1H), 5.90 (d, *J* = 14.7 Hz, 1H), 5.75 (d, *J* = 1.7 Hz, 1H), 5.57 (d, *J* = 12.1 Hz, 1H), 1.25 (s, 9H), 1.24 (s, 9H). ¹³C NMR (CDCl₃, 100 MHz): δ 166.1, 165.5, 160.4, 155.6, 138.8, 133.8, 117.3, 114.2, 110.8, 105.4, 103.3, 98.9, 41.4, 41.3, 36.0, 35.6, 31.0, 29.7, 27.9, 27.8, 26.8. HRMS (ESI⁺): calcd for C₄₀H₄₉N₂O₃ (M + H)⁺ 605.3738; found 605.3744. Anal. Calcd for C₄₀H₄₈N₂O₃: C 79.43, H 8.00, N 4.63. Found: C 79.68, H 8.21, N 4.45.

2-(2,6-Bis((E)-3-(2,6-di-tert-butyl-4H-pyran-4-ylidene)prop-1-enyl)-4H-pyran-4-ylidene)-1,3-indanedione (10b). Chromatography eluent: hexane/AcOEt 9:1, then hexane/AcOEt 8.5:1.5 and finally hexane/AcOEt 8:2. Yield: dark blue solid (55 mg; 17%). Mp 135–138 °C (dec). IR (Nujol, cm⁻¹) 1668 (C=O), 1613 (C=C). ¹H NMR (CDCl₃, 400 MHz): δ 8.33 (s, 1H), 7.69–7.67 (m, 1H), 7.53–7.45 (m, 2H), 6.19 (d, *J* = 1.7 Hz, 1H),

6.07 (d, $J = 14.7$ Hz, 1H), 5.75 (d, $J = 1.7$ Hz, 1H), 5.60 (d, $J = 12.1$ Hz, 1H), 1.25 (s, 9H), 1.21 (s, 9H). ^{13}C NMR (CDCl_3 , 100 MHz): δ 193.0, 165.7, 165.1, 162.4, 149.0, 140.6, 138.0, 133.0, 132.4, 120.6, 116.1, 111.3, 106.1, 105.3, 98.9, 35.9, 35.5, 27.9, 27.7. HRMS (ESI^+): calcd for $\text{C}_{46}\text{H}_{53}\text{O}_5$ ($\text{M} + \text{H}$) $^+$ 685.3888; found 685.3891. Anal. Calcd for $\text{C}_{46}\text{H}_{52}\text{O}_5$: C 80.67, H 7.65. Found: C 80.41, H 7.79.

5-(2,6-Bis((*E*)-3-(2,6-di-*tert*-butyl-4*H*-pyran-4-ylidene)prop-1-enyl)-4*H*-pyran-4-ylidene)-1,3-diethyl-2-thioxodihydropyrimidine-4,6-dione (10c). Chromatography eluent: hexane/AcOEt (9:1). Yield: dark blue solid (70 mg; 20%). Mp 260–265 °C (dec). IR (Nujol, cm^{-1}) 1661 (C=O), 1105 (C=S). ^1H NMR (CDCl_3 , 400 MHz): δ 8.65 (s, 1H), 7.55 (dd, $J = 14.7$ Hz, $J' = 12.2$ Hz, 1H), 6.22 (d, $J = 1.7$ Hz, 1H), 6.08 (d, $J = 14.7$ Hz, 1H), 5.79 (d, $J = 1.7$ Hz, 1H), 5.62 (d, $J = 12.2$ Hz, 1H), 4.62 (q, $J = 6.9$ Hz, 2H), 1.33 (t, $J = 6.9$ Hz, 3H), 1.26 (s, 9H), 1.22 (s, 9H). ^{13}C NMR (CDCl_3 , 100 MHz): δ 177.1, 166.2, 165.7, 162.9, 161.9, 156.1, 139.2, 134.4, 115.5, 111.4, 110.9, 105.6, 99.2, 94.7, 43.2, 36.0, 35.6, 27.9, 27.8, 12.6. HRMS (ESI^+): calcd for $\text{C}_{45}\text{H}_{59}\text{N}_2\text{O}_5\text{S}$ ($\text{M} + \text{H}$) $^+$ 739.4139; found 739.4124. Anal. Calcd for $\text{C}_{45}\text{H}_{58}\text{N}_2\text{O}_5\text{S}$: C 73.14, H 7.91, N 3.79. Found: C 72.92, H 7.69, N 3.95.

Compounds 11a–c. General Procedure. 11a–c were prepared analogously to 9a–c, but starting from 0.5 mmol of (*E*)-4-(2,6-di-*tert*-butyl-4*H*-pyran-4-ylidene)-but-2-enal (4). Reaction time was 3–5 h.

(*E,E*)-[2-*tert*-Butyl-6-(5-(2,6-di-*tert*-butyl-4*H*-pyran-4-ylidene)penta-1,3-dienyl)-4*H*-pyran-4-ylidene]malononitrile (11a). Reaction time: 3 h 40 min. After cooling, the precipitate was isolated by filtration, washed with cold pentane and dried. Dark violet solid (173 mg; 76%). Mp 152–153 °C. IR (Nujol, cm^{-1}) 2197 (C≡N). ^1H NMR (CDCl_3 , 400 MHz): δ 7.17 (dd, $J = 14.9$ Hz, $J' = 11.6$ Hz, 1H), 6.94 (dd, $J = 14.0$ Hz, $J' = 12.3$ Hz, 1H), 6.50 (d, $J = 2.0$ Hz, 1H), 6.46 (d, $J = 2.0$ Hz, 1H), 6.19 (dd, $J = 14.0$ Hz, $J' = 11.6$ Hz, 1H), 6.11 (d, $J = 1.7$ Hz, 1H), 5.99 (d, $J = 14.9$ Hz, 1H), 5.70 (d, $J = 1.7$ Hz, 1H), 5.53 (d, $J = 12.3$ Hz, 1H), 1.35 (s, 9H), 1.25 (s, 9H), 1.20 (s, 9H). ^{13}C NMR (CDCl_3 , 100 MHz): δ 171.6, 165.4, 164.8, 160.4, 156.5, 139.9, 137.7, 136.9, 124.4, 116.1, 116.0, 111.8, 105.2, 104.9, 102.1, 98.9, 56.9, 36.5, 35.8, 35.5, 28.1, 27.9, 27.7 ppm. HRMS (ESI^+): calcd for $\text{C}_{30}\text{H}_{37}\text{N}_2\text{O}_2$ ($\text{M} + \text{H}$) $^+$ 457.2850; found 457.2749. Anal. Calcd for $\text{C}_{30}\text{H}_{36}\text{N}_2\text{O}_2$: C 78.91, H 7.95, N 6.13. Found: C 79.14, H 7.68, N 6.30.

(*E,E*)-2-(2-*tert*-Butyl-6-(5-(2,6-di-*tert*-butyl-4*H*-pyran-4-ylidene)penta-1,3-dienyl)-4*H*-pyran-4-ylidene)-1,3-indanedione (11b). Reaction time: 3 h. Chromatography eluent: hexane/AcOEt (85:15). Yield: dark violet solid (211 mg; 79%). Mp 125–127

°C. IR (Nujol, cm^{-1}) 1650 (C=O). ^1H NMR (CDCl_3 , 400 MHz): δ 8.38 (d, $J = 1.6$ Hz, 1H), 8.35 (d, $J = 1.6$ Hz, 1H), 7.73–7.68 (m, 2H), 7.59–7.55 (m, 2H), 7.22 (dd, $J = 15.0$ Hz, $J' = 11.6$ Hz, 1H), 6.95 (dd, $J = 14.0$ Hz, $J' = 12.2$ Hz, 1H), 6.23 (dd, $J = 14.0$ Hz, $J' = 11.6$ Hz, 1H), 6.16 (d, $J = 15.0$ Hz, 1H), 6.10 (d, $J = 1.5$ Hz, 1H), 5.69 (d, $J = 1.5$ Hz, 1H), 5.53 (d, $J = 12.2$ Hz, 1H), 1.39 (s, 9H), 1.23 (s, 9H), 1.18 (s, 9H). ^{13}C NMR (CDCl_3 , 100 MHz): δ 192.9, 173.3, 165.1, 164.4, 162.8, 149.6, 140.6, 140.5, 138.7, 136.8, 136.1, 132.8, 125.0, 120.9, 120.8, 118.1, 111.9, 107.3, 106.8, 105.1, 103.4, 98.8, 36.8, 35.8, 35.4, 28.3, 27.9, 27.7. HRMS (ESI^+): calcd for $\text{C}_{36}\text{H}_{41}\text{O}_4$ ($\text{M} + \text{H}$) $^+$ 537.2999; found 537.2981. Anal. Calcd for $\text{C}_{36}\text{H}_{40}\text{O}_4$: C 80.56, H 7.51. Found: C 80.43, H 7.34.

(*E,E*)-5-[2-*tert*-butyl-6-(5-(2,6-di-*tert*-butyl-4*H*-pyran-4-ylidene)penta-1,3-dienyl)-4*H*-pyran-4-ylidene]-1,3-diethyl-2-thioxodihydropyrimidine-4,6-dione (11c). Reaction time: 5 h. Purified by repeated column chromatography (first chromatography eluent: hexane/AcOEt (9:1); second chromatography eluent: CH_2Cl_2 /hexane (9:1)). Yield: dark blue solid (186 mg; 63%). Mp 113–114 °C. IR (Nujol, cm^{-1}) 1672 (C=O), 1108 (C=S). ^1H NMR (CDCl_3 , 400 MHz): δ 8.81 (d, $J = 1.9$ Hz, 1H), 8.75 (d, $J = 1.9$ Hz, 1H), 7.32 (dd, $J = 14.9$ Hz, $J' = 11.5$ Hz, 1H), 7.02 (dd, $J = 13.4$ Hz, $J' = 12.2$ Hz, 1H), 6.25–6.15 (m, 3H), 5.72 (d, $J = 1.8$ Hz, 1H), 5.56 (d, $J = 12.2$ Hz, 1H), 4.60 (q, $J = 6.9$ Hz, 4H), 1.42 (s, 9H), 1.32 (t, $J = 6.9$ Hz, 6H), 1.26 (s, 9H), 1.20 (s, 9H). ^{13}C NMR (CDCl_3 , 100 MHz): δ 177.5, 173.6, 165.6, 165.0, 163.8, 161.9, 157.8, 140.5, 138.2, 137.3, 124.9, 117.6, 112.1, 117.7, 107.8, 105.4, 99.1, 96.4, 43.3, 37.1, 35.9, 35.6, 28.5, 27.9, 27.8, 12.6. HRMS (ESI^+): calcd for $\text{C}_{35}\text{H}_{47}\text{N}_2\text{O}_4\text{S}$ ($\text{M} + \text{H}$) $^+$ 591.3251; found 591.3230. Anal. Calcd for $\text{C}_{35}\text{H}_{46}\text{N}_2\text{O}_4\text{S}$: C 71.15, H 7.85, N 4.74. Found: C 70.87, H 7.64, N 4.92.

Acknowledgment. Financial support from MICINN-FEDER (CTQ2008-02942 and MAT2008-06522C02-02) and Gobierno de Aragón-Fondo Social Europeo (E39) is gratefully acknowledged. Predoctoral fellowships to E. Galán (CSIC, JAE 2008) and R. Alicante (FPI BES 2006-12104) are also acknowledged.

Supporting Information Available: General experimental methods, NMR and UV–vis spectra of new compounds, NLO measurements, computed energies and Cartesian coordinates of optimized geometries. This material is available free of charge via the Internet at <http://pubs.acs.org>.